

Received 28 November 2022, accepted 31 December 2022, date of publication 5 January 2023,  
date of current version 10 January 2023.

Digital Object Identifier 10.1109/ACCESS.2023.3234577

## RESEARCH ARTICLE

# Dynamic Optical Wireless Power Transfer for Electric Vehicles

**DINH HOA NGUYEN**<sup>1</sup>, (Senior Member, IEEE)

International Institute for Carbon-Neutral Energy Research (WPI-I2CNER), and the Institute of Mathematics for Industry (IMI), Kyushu University, Fukuoka 819-0395, Japan

e-mail: hoa.nd@i2cner.kyushu-u.ac.jp

**ABSTRACT** This research proposes and analyzes a dynamic optical wireless power transfer (OWPT) system for wireless charging of aerial and ground electric vehicles (EVs). In this system, an overhead facility is proposed to locate laser transmitters, renewable energy resources, and energy storage devices. There are laser transmitters on the facility's roof pointing upward to wirelessly charge aerial EVs, while the other laser transmitters on the facility's ceiling pointing downward to wirelessly charge ground EVs. All laser transmitters are able to rotate around the normal direction to track and continuously charge aerial and ground EVs while they are moving, due to the equipped tracking cameras. Analytical mathematical formulas are then derived for the wirelessly transmitted power and energy. Based on those formulas, the unique existence of maximum power and energy points are proved. Furthermore, those maximum points are shown to be inversely linearly dependent on the environment attenuation coefficient, i.e. on weather conditions. Numerical simulations are carried out to validate and illustrate the obtained theoretical results. Finally, implications of those results on the design of ground EVs are introduced, based on which a comparison with another wireless power transfer technology reveals that the proposed dynamic OWPT system is more effective.

**INDEX TERMS** Optical wireless power transfer, electric vehicle, wireless charging, smart infrastructure, sustainability.

## I. INTRODUCTION

Transportation, together with power generation, are the two sectors that emit largest portions of greenhouse gases (GHG). Therefore, as nations around the globe are trying hard to significantly reduce GHG emissions in order to ease the global warming and severe effects of climate changes, transportation electrification is emerged as one of critical solutions. Electrified vehicles can be powered utilizing different ways, e.g. direct use of electricity via batteries or supercapacitors, or indirect use of electricity via fuel cells, etc.

For electric vehicles (EVs) run directly on electricity stored in batteries or supercapacitors, currently their charging and discharging are mostly conducted by connecting to charging stations via electric wires (cables). There are

major disadvantages of this wired charging and discharging method. First, EVs must be stopped while being charged or discharged, hence hindering their mobility and flexibility. Second, most of current wired charging stations require several hours for fully charging EVs, which is only suitable for overnight charging at homes or daytime charging at offices without leaves. Compared to several minutes of refueling gasoline vehicles, this is a huge difference, causing discomfort and inconvenience to users. Last but not least, there are concerns on fire or explosion caused by wired charging, especially as it is made during a long time.

To overcome the disadvantages of wired charging mentioned above, wireless power transfer (WPT) is a promising approach [1], [2], [3], [4], in which no wires are needed between EVs and charging devices. There are different WPT methods depending on the employed technologies, e.g. inductive WPT (IWPT) [5], [6], [7], capacitive WPT (CWPT) [8], optical WPT (OWPT) [9], [10], [11], and

The associate editor coordinating the review of this manuscript and approving it for publication was N. Prabaharan<sup>1</sup>.

microwave WPT (MWPT) [12], [13], [14], etc. Currently, IWPT using resonant circuits at the primary (transmitter) and secondary (receiver) sides, also called resonant IWPT, has received much attention for wireless charging of ground EVs, partly due to their high power conversion efficiency (PCE). However, in this resonant IWPT technology, transmitting distance is short, where coils that are equipped on ground EVs should be close to those embedded under road lanes or those in wireless charging pads. A similar shortcoming exists for aerial and maritime EVs using the resonant IWPT method.

In order to obtain longer transmitting distances, OWPT and MWPT should be employed, but at the cost of lower PCEs. Nevertheless, to efficiently transmit a high amount of energy, sizes of MWPT systems are much larger than that of OWPT systems, at the same output power of transmitters. Thus, MWPT may be more suitable for space applications, for instance, for being used in space solar power systems (SSPS) in which giant solar arrays collect solar power in outer space and then the collected solar energy is transmitted to the ground on Earth via microwave beams. As such, our focus is on the use of OWPT for EV wireless charging systems.

Recently, PCEs of solar cells have been greatly improved including that to be used with monochromatic lasers, e.g. the record 68.9% efficiency reported in [15]. Moreover, the transmitting distance of laser lights could be in the scale of kilometers that cannot be achieved with resonant IWPT or CWPT technologies. Therefore, laser-based OWPT becomes an emerging technology for wirelessly charging electric and electronic devices including batteries and supercapacitors in EVs. Feasibility assessment of laser-based wireless charging of unmanned aerial vehicles (UAVs) was conducted and shown to be viable in [16], where previous works on this topic were also reviewed. Recent field tests, e.g. [17], [18], and [19], shows the viability and promising upscale of OWPT to a variety of systems and applications including wireless charging of 5G base stations, and aerial and ground EVs. Note, however, that there have been no reports on the details of such systems, nor their theoretical parts. In addition, those OWPT systems were used for stationary objects or hovering drones.

In the current research, we propose a novel laser-based dynamic OWPT system capable of wirelessly charging both moving aerial and ground EVs. This system includes a set of laser transmitters located on an overhead facility. Those laser transmitters are rotated to track and send power to EVs while they are moving, are pointed downward and upward for wireless charging of ground and aerial EVs, respectively. The lane under the locations of those laser transmitters is called an optical wireless charging lane (OWCL). Then this system is theoretically analyzed to contribute the following to the literature.

- Analytically mathematical formulas for the wirelessly transmitted power and energy to ground and aerial EVs as they are moving. These formulas clearly show the dependence of transmitted power and energy on transmitting distance and environment conditions.

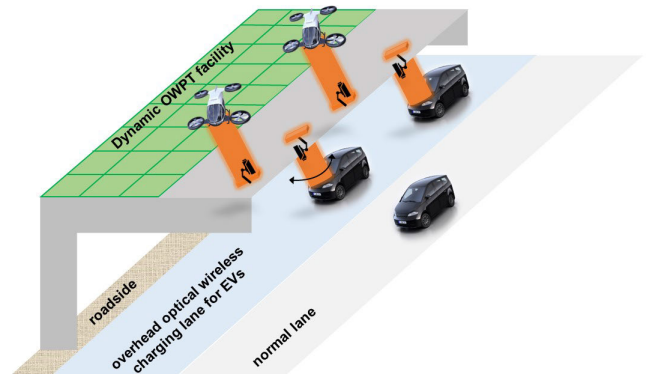


FIGURE 1. Illustration for optical wireless charging of EVs.

- Proof for the unique existence of the maximum power and energy points of the proposed laser-based dynamic OWPT system.
- Proof for the inversely linearly dependence of the maximum power and energy points on the environment attenuation coefficient.

The rest of this paper is organized as follows. A description and a mathematical model of the overhead laser-based dynamic OWPT for moving EVs are presented in Section II. Then the features of wirelessly transmitted power and energy on the transmitting distance are studied in Section III, followed by a numerical example to illustrate derived theoretical results. Next, further insights on the usefulness of the derived theoretical results to practical laser-based OWPT system design are given in Section IV. Finally, the conclusion and future research directions are presented in Section V.

## II. MATHEMATICAL MODEL OF LASER-BASED DYNAMIC OWPT SYSTEM FOR EVs

### A. DESCRIPTION OF THE PROPOSED LASER-BASED OWPT SYSTEM

The current work studies the dynamic wireless charging of EVs in which different types of EVs are applicable including those moving on the ground and flying in the sky. In order to obtain a unified infrastructure, we propose an overhead laser-based OWPT facility, as illustrated in Figure 1, where laser energy is transmitted to solar cells attached on ground and aerial EVs.

The laser transmitters can be rotated within a range  $[-\varphi_m, \varphi_m]$  around the normal (perpendicular) direction to dynamically charge EVs while they are moving, where  $\varphi_m \in (0, \pi/2)$ . These laser transmitters can track and rotate to follow EVs by using suitable cameras, but details are ignored here because it is not the main focus in this work. The safety of laser radiation to users and other pass-by objects can be guaranteed by employing additional technologies, e.g. a virtual safety shutoff ring surrounding the laser beams [17], or by establishing a resonant cavity between transmitters and receivers so that the laser transmission will be stopped if any object is existed in the transmission path (see, e.g. [20]).

Furthermore, optical lenses are used to widen the laser beam width while making laser beams collimated and top-hat rectangular. The advantages of top-hat rectangular laser beams are to obtain a uniformly distributed power density, unlike Gaussian beams, and to better fit for solar cells than circular beams.

Renewable energy sources (RESs), e.g. solar panels, wind turbines, and energy storage, e.g. batteries, are co-located with the overhead facility to supply clean energy for this laser-based OWPT system. When power from these RESs and batteries are not enough, grid supply will be utilized.

Considering realistic issues of dense population, infrastructures, and buildings in urban environments, the proposed laser-based dynamic OWPT system is most suitable for highways, suburban areas, tunnels, and underground (for ground EVs and trains). It can also be employed for indoor systems, e.g. for wireless charging of robots, forklifts, etc. operated in autonomous factories or manufacturing systems. A more detailed analysis with suggestions for EV design will be provided in Section IV.

## B. MATHEMATICAL MODEL FOR SYSTEM ENERGY EFFICIENCY

Let  $n_\ell$  be the number of overhead OWPT laser transmitters and  $\varphi_m$  [rad] be the maximum rotating angle of each laser transmitter around the perpendicular direction. As an EV is moving within the angular range  $[-\varphi_m, \varphi_m]$  of a laser transmitter, its angular position with respect to the perpendicular direction is denoted by  $\varphi$ , hence  $\varphi \in [-\varphi_m, \varphi_m]$ . Furthermore, let  $P_\ell$  be the output power of a laser energy transmitter,  $\eta_{env}$  be the OWPT when a laser beam is transmitted through the environment,  $\eta_l$  be the efficiency of the utilized optical lenses, and  $\eta_e$  be the laser-to-electricity conversion efficiency of EV's solar cells. Then the power each EV receives at a time instant  $t$  is

$$P_c(t) = P_\ell \eta_{env} \eta_l \eta_e \cos \varphi. \quad (1)$$

The environment for OWPT here is the air through which the laser energy transmission efficiency is an exponentially decaying function of the transmitting distance, following the Beer-Lambert law,

$$\eta_{env} = e^{-\sigma \ell}. \quad (2)$$

In (2),  $\ell$  [km] is the transmitting distance to the EV, and  $\sigma$  [ $\text{km}^{-1}$ ] is the attenuation coefficient showing how laser energy is lost by the diffraction, absorption and scattering, due to the suspended molecules in the environment [21], [22]. As such,  $\sigma$  is dependent on the laser wavelength and the environment characteristics. A detailed discussion on how to evaluate  $\sigma$  was given in [23]. The distance  $\ell$  is equal to  $h/\cos \varphi$ , where  $h$  [km] is the distance from the laser transmitter to the solar cells on top of an EV at the normal direction. Hence, the power each EV receives at a time instant  $t$  is

$$P_c(t) = P_\ell \eta_l \eta_e e^{-\sigma \ell} \cos \varphi = P_\ell \eta_l \eta_e h \frac{e^{-\sigma \ell}}{\ell}. \quad (3)$$

Assume that the distance  $h$  is a constant during the moving of EVs, then the accumulated charging power for the EV is computed by

$$P_c = 2 \int_h^{h_m} P_\ell \eta_l \eta_e h \frac{e^{-\sigma \ell}}{\ell} d\ell = 2P_\ell \eta_l \eta_e h \int_h^{h_m} \frac{e^{-\sigma \ell}}{\ell} d\ell, \quad (4)$$

with  $h_m \triangleq h/\cos \varphi_m$ .

*Proposition 1:* For  $h > 0$ ,  $\sigma > 0$ ,  $0 < \varphi_m < \pi/2$ , the integral  $\int_h^{h_m} \frac{e^{-\sigma \ell}}{\ell} d\ell$  is a monotonically decreasing function of  $h$ .

*Proof:* Let us denote  $g(\ell) \triangleq \int \frac{e^{-\sigma \ell}}{\ell} d\ell$ , then

$$\int_h^{h_m} \frac{e^{-\sigma \ell}}{\ell} d\ell = g(h_m) - g(h).$$

Taking derivative with respect to  $h$  for the both sides of the equation above, we get

$$\frac{\partial g(h_m)}{\partial h} - \frac{\partial g(h)}{\partial h} = \frac{e^{-\frac{\sigma h}{\cos \varphi_m}}}{h} - \frac{e^{-\sigma h}}{h}. \quad (5)$$

Since  $0 < \cos \varphi_m < 1$ ,  $\sigma > 0$ , and  $h > 0$ , the right hand side of (5) is strictly negative. As such, the integral  $\int_h^{h_m} \frac{e^{-\sigma \ell}}{\ell} d\ell$  is a monotonically decreasing function of  $h$ . ■

Unfortunately, there is no analytical and finite solution for the integral in (4). Therefore, the integral in (4) should be numerically computed, for example, utilizing adaptive quadrature methods. On the other hand, using the well-known mathematical concept of the exponential integral function  $\text{Ei}(x) \triangleq \int_{-\infty}^x \frac{e^z}{z} dz$ , the wirelessly transmitted power in (4) can be rewritten as follows,

$$\begin{aligned} P_c &= 2P_\ell \eta_l \eta_e h \int_{-\sigma h}^{-\sigma h_m} \frac{e^\ell}{\ell} d\ell \\ &= 2P_\ell \eta_l \eta_e h [\text{Ei}(-\sigma h_m) - \text{Ei}(-\sigma h)]. \end{aligned} \quad (6)$$

Next, the energy each EV receives is computed by

$$E_c = n P_c t_{charge}, \quad (7)$$

where  $n \leq n_\ell$  is the number of laser transmitters that an EV passes through and  $t_{charge}$  is the charging time, i.e. the time that an EV moves on the OWCL. Now assuming that when traveling along the OWCL, the EV's velocity, denoted by  $v_{wpt}$ , can be controlled to be unchanged, then this charging time is equal to  $\frac{2h \tan \varphi_m}{v_{wpt}}$ . Accordingly, the wireless charging energy sent to an EV is,

$$\begin{aligned} E_c &= n P_c \frac{2h \tan \varphi_m}{v_{wpt}} \\ &= 4n P_\ell \eta_l \eta_e \frac{\tan \varphi_m}{v_{wpt}} h^2 [\text{Ei}(-\sigma h_m) - \text{Ei}(-\sigma h)]. \end{aligned} \quad (8)$$

**III. CHARACTERIZATION OF THE PROPOSED LASER-BASED DYNAMIC OWPT SYSTEM FOR EVs**

**A. EXISTENCE OF EXTREME POINTS**

It can be observed from Eq. (4) and Eq. (7) that the wirelessly transmitted power and energy to an EV are functions of the distance  $h$ , the rotating angle  $\varphi_m$ , and the speed  $v_{wpt}$  of EVs. In reality, the angle  $\varphi_m$  is selected for the laser sources and is fixed, whereas the vehicle speed  $v_{wpt}$  on the OWCL is also requested to be fixed, hence the wirelessly transmitted power and energy can be considered to be solely dependent on the distance  $h$ . Note that  $h$  is in fact the difference between the height of an EV and that of the overhead laser sources. In practice, the height of the overhead OWPT facility is fixed, while the heights of different EVs, e.g. electric buses, electric sedans, electric SUVs, etc., could be distinct. Therefore, in the following theorem we show the maximum points of  $P_c$  and  $E_c$ , how to determine them, and how they are dependent on the environment attenuation coefficient  $\sigma$ .

*Theorem 1:* For any  $h > 0$ ,  $\sigma > 0$ ,  $0 < \varphi_m < \pi/2$ , there exist a unique constant  $h^* \in \left(\frac{\cos \varphi_m}{\sigma}, \frac{1}{\sigma}\right)$  and a unique constant  $\tilde{h}^* \in \left(\frac{2 \cos \varphi_m}{\sigma}, \frac{2}{\sigma}\right)$  at which  $\left.\frac{\partial P_c}{\partial h}\right|_{h=h^*} = 0$  and  $\left.\frac{\partial E_c}{\partial h}\right|_{h=\tilde{h}^*} = 0$ . These points  $h^*$  and  $\tilde{h}^*$  are the maximum power and energy points of the proposed laser-based dynamic OWPT system, respectively. Moreover, let  $g(y) \triangleq \text{Ei}(-y) + e^{-y}$ ,  $q(y) \triangleq 2\text{Ei}(-y) + e^{-y}$ , and  $\alpha \triangleq 1/\cos \varphi_m$ , then

- (i)  $h^* \sigma = y^*$ , where  $y^*$  is a constant which is the unique solution of the equation  $g(\alpha y) - g(y) = 0$ ; and
- (ii)  $\tilde{h}^* \sigma = \tilde{y}^*$ , where  $\tilde{y}^*$  is constant which is the unique solution of the equation  $q(\alpha y) - q(y) = 0$ .

As such, the maximum power and energy points are inversely linear functions of the environment attenuation coefficient  $\sigma$ .

*Proof:* See the Appendix. ■

The results of Proposition 1 and Theorem 1 will be illustrated via numerical examples in Section III-D.

*Remark 1:* The maximum power and energy points  $h^*$  and  $\tilde{h}^*$  in Theorem 1 are different, where the former is usually smaller than the later, due to their belonging intervals. Thus, system designers should choose the transmitting distance corresponding to one of those points and other realistic requirements.

*Remark 2:* In the context of static optical wireless charging, ground EVs are stopped, while aerial EVs are hovering or stopped on dedicated places over laser transmitters. As such, OWPT is made at the normal direction, and hence, the instantaneous power an EV receives is

$$P_c = P_\ell \eta_l \eta_e e^{-\sigma h}. \tag{9}$$

The energy amount an EV receives during a time period  $\mathbb{T}$  is

$$E_c = P_c \mathbb{T} = P_\ell \eta_l \eta_e e^{-\sigma h} \mathbb{T}. \tag{10}$$

Therefore, the wirelessly transmitted power and energy are exponentially decaying functions of the transmitting distance  $h$ . This implies that EVs should be as close as

possible to laser transmitters, taking into account the safety issues. We can also see that characteristics of the static optical wireless charging are much simpler than that of the dynamic optical wireless charging shown in Theorem 1.

*Remark 3:* Although the results in Theorem 1 are developed for fixed laser transmitters, they are theoretically applicable for more advanced contexts of moving laser transmitters as well. In particular, laser transmitters may be equipped on a moving aerial or ground EV to wirelessly charge another moving aerial or ground EV. This wireless charging between moving EVs was suggested in [4].

**B. DETERMINATION OF EXTREME POINTS**

As can be seen in the Appendix,  $g(\alpha y) - g(y)$  is a monotonically decreasing function in the interval  $(\frac{1}{\alpha}, 1)$ , and  $(g(\alpha y) - g(y))|_{y=\frac{1}{\alpha}} > 0$ ,  $(g(\alpha y) - g(y))|_{y=1} < 0$ . Hence, the well-known bisection method is suitable to determine  $h^*$ . Similar observations are applied for the maximum energy point  $\tilde{h}^*$ . This will be illustrated via numerical simulations in Section III-D.

If one wants to increase the convergence speed to the solution, the ITP (Interpolation-Truncation-Projection) method [24] can be used. This ITP method achieves a super-linear convergence speed compared to the linear convergence rate of the bisection method, however at each iteration one needs to perform more computational efforts (see [24] for details).

**C. PROVISION OF GRID ANCILLARY SERVICES**

From the grid viewpoint, both the proposed laser-based dynamic OWPT system and EVs can be regarded as distributed energy resources (DERs). With on-site RESs and energy storage devices, this overhead laser-based dynamic OWPT system can generate energy on its own and send the redundant energy to the grid, while consuming energy from the grid when needed. Hence, the proposed dynamic OWPT system can provide ancillary services to the grid, e.g. supply-demand balancing, frequency control, etc.

As an example, when power supply is more than power demand in the grid, EVs and energy storage devices of the proposed dynamic OWPT system can take charging to consume the power mismatch to avoid the economic loss due to curtailments. On the contrary, when power supply is less than power demand, on-site RESs and storage devices of the proposed dynamic OWPT system can be utilized to supply power back to the grid to circumvent the economic loss and discomfort due to load shedding. In both scenarios, appropriate power prices should be devised to incentivize the participation of EVs and wireless charging systems. More specifically, ancillary service price is smaller or greater than market price when the power mismatch is positive or negative, respectively. Examples of an energy trading framework between EVs and the wireless charging lane were presented in our previous works [25], [26].



### D. NUMERICAL SIMULATIONS

In this section, we numerically verify theoretical results introduced in Section III-A under different scenarios. In particular, how different weather conditions affect to the wirelessly transmitted optical power and energy will be simulated. All simulations are conducted in Matlab 2016a installed on a desktop computer with an Intel i7-6700K 4GHz 64-bit CPU and a 64 GB RAM.

We assume that laser transmitters are located 10 m above the ground with their maximum rotating angle  $\varphi_m$  to be  $\pi/4$  rad. Under these assumptions, the traveling distance under which an EV receives optical wireless charging is  $2h \tan \varphi_m = 2h$ . Furthermore, suppose that GaAs solar cells are used as optical receivers, which could have a very high energy conversion efficiency of 68.9% under a 858 nm monochromatic laser light [15]. Since all other parameters such as  $P_\ell, n, \eta_c, v_{wpt}$  are constant, we will verify how the variations of the terms related to  $h$  in Eq. (4) and Eq. (7) affect to the wirelessly transmitted power and energy.

Next, using the results of Theorem 1 and the bisection method, we derive  $y^* = 0.8452$  and  $\tilde{y}^* = 1.7075$ . As such, we can immediately determine the maximum power and energy point at each value of  $\sigma$ , i.e. at each transmitting environment condition. This is illustrated for different scenarios below.

#### 1) DYNAMIC OWPT UNDER HAZE ATMOSPHERE

First, we simulate how the proposed DOWPT system works under the haze weather condition, in which the value of  $\sigma$  is typically equal to 1 [23]. Simulation results are depicted in Figure 2, revealing the same characteristics of the integral in (4) and (7) with respect to the distance  $h_i$  as that in the previous scenario. On the other hand, the wirelessly transmitted power is monotonically decreasing with the distance  $h$  when  $h \geq h^*$ , and is monotonically increasing as  $0 < h \leq h^*$ , where  $0.7071 \approx \frac{\cos \varphi_m}{\sigma} < h^* < \frac{1}{\sigma} = 1$ . Furthermore, the wirelessly transmitted energy can be observed in Figure 2 to be monotonically decreasing when the distance  $h \geq \tilde{h}^*$  km, and is monotonically increasing as  $0 < h \leq \tilde{h}^*$ , with  $1.4142 \approx \frac{2 \cos \varphi_m}{\sigma} < \tilde{h}^* < \frac{2}{\sigma} = 2$ . All of these observations are coincided with the results of Proposition 1 and Theorem 1.

Consequently, the maximum power point derived from Theorem 1 and the bisection method is 0.8452 km which is found after 51 iterations, whereas it is 0.845 km in Figure 2. On the other hand, the maximum energy point is found to be 1.7075 km after 101 iterations of the bisection method, while its value in Figure 2 is 1.708 km. Clearly, the bisection method gives precise maximum power and energy points of the proposed laser-based dynamic OWPT system. Similar precisions are also observed for different weather conditions in the next sections, hence will be omitted for brevity.

#### 2) DYNAMIC OWPT UNDER CLEAR ATMOSPHERE

Next, the attenuation coefficient  $\sigma$  is assumed to be 0.1 which is corresponding to clear atmosphere condition [23]. Simulation results are shown in Figure 3. As can be seen in Figure 3,

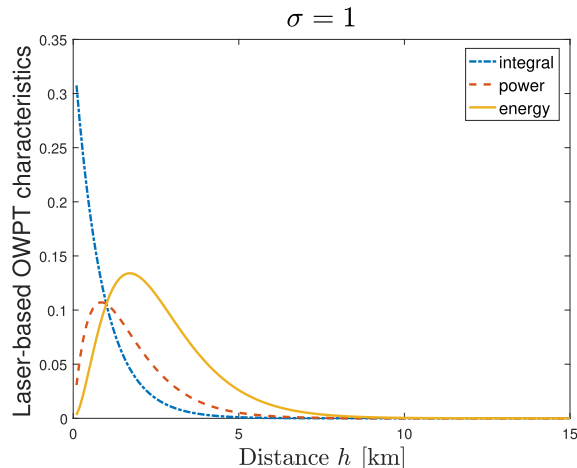


FIGURE 2. Wirelessly transmitted power and energy under haze weather condition ( $\sigma = 1$ ).

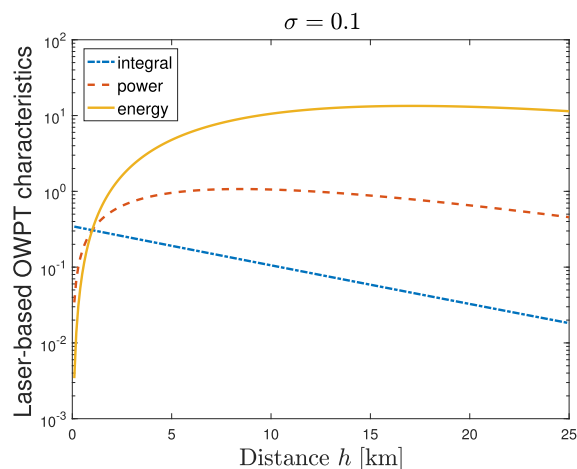


FIGURE 3. Wirelessly transmitted power and energy under clear atmosphere ( $\sigma = 0.1$ ).

the integral in (4) and (7) is monotonically decreasing with respect to the distance  $h$ . In addition, the accumulated power wirelessly transmitted to EVs is monotonically increasing when  $h$  is in between 0 and some  $h^*$ , and is monotonically decreasing as  $h \geq h^*$ , where  $7.0711 \approx \frac{\cos \varphi_m}{\sigma} < h^* < 1/\sigma = 10$ . Likewise, the wirelessly transmitted energy to EVs is monotonically increasing when  $0 < h \leq \tilde{h}^*$ , and is monotonically decreasing as  $h \geq \tilde{h}^*$ , with  $14.1421 \approx \frac{2 \cos \varphi_m}{\sigma} < \tilde{h}^* < 2/\sigma = 20$ . These are consistent with the results of Proposition 1 and Theorem 1.

We can observe from simulation results in Figure 3 that the maximum power point occurs at a transmitting distance of a few kilometers, and that for the maximum energy point is much further, nearly 18 kilometers. While these are theoretically attractive, they are difficult to be applied in many realistic situations, due to the existence of obstacles, especially in urban environments.

#### 3) DYNAMIC OWPT UNDER FOG ATMOSPHERE

Lastly, we consider the fog weather condition with typical value  $\sigma = 10$  [23]. Simulation results in this scenario

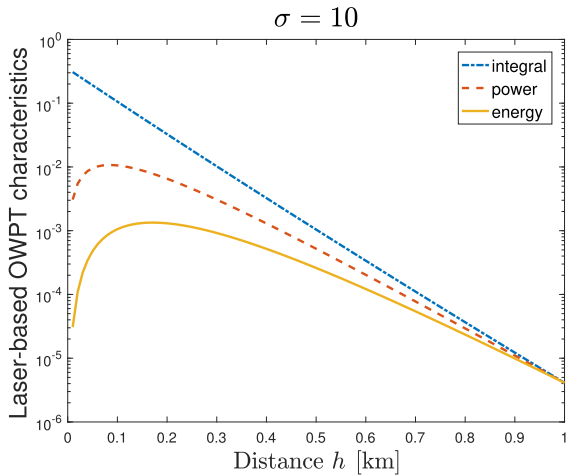


FIGURE 4. Wirelessly transmitted power and energy under fog weather condition ( $\sigma = 10$ ).

are displayed in Figure 4, showing that both the wirelessly transmitted power and energy are rapidly vanished even when the transmitting distance is less than 1 km. This is consistent with the results of Theorem 1 and Theorem 1, since the wirelessly transmitted power and energy are monotonically decreasing function of the transmitting distance  $h$  when  $h \geq \frac{1}{\sigma} = 0.1$  km and when  $h \geq \frac{2}{\sigma} = 0.2$  km, respectively.

We can observe clearly from three scenarios depicted in Figures 3–4 that the amounts of laser power and energy wirelessly transmitted to EVs are greatly reduced as the value of  $\sigma$  is increased much, i.e. when the atmospheric condition becomes worse. Simultaneously, the transmitting distance is quickly reduced as the atmospheric condition is worsen to be around 100 meters and less than 200 meters for the maximum power and energy point, respectively. These distances are smaller than that of 325 meters in the field test of stationary OWPT [18].

#### IV. IMPLICATIONS ON LASER-BASED DYNAMIC OWPT DESIGN FOR MOVING GROUND EVs

Based on the theoretical analysis on laser-based dynamic OWPT in Section III and numerical simulations in Section III-D, this sections proposes a more detailed design of overhead laser-based dynamic OWPT systems for ground EVs. It is anticipated that future ground EVs will be attached with solar arrays on their roof, bonnet, trunk, and body for the maximum harvest of light energy from the sun and OWPT charging systems.

Here, we propose that the overhead laser transmitters are located at the same height from the ground as that for traffic tunnels, which is around 10 m. Then OWPT is made from those overhead laser sources to solar arrays attached on top of EVs’ bonnet, as illustrated in Figure 5, due to the following reasons. First, some EVs, e.g. electric sport utility vehicles (SUVs), have no or very small trunks. Second, a vehicle bonnet has lower height than its roof and trunk (if exists), hence has a larger distance  $h$  to overhead laser transmitters. Note that the distance  $h$  with the above

assumption of laser transmitters’ height is less than 10 m. Therefore, EVs will get more wirelessly transmitted laser power and energy, as theoretically shown in Theorem 1 and numerically simulated in Section III-D, even in different atmospheric conditions. Third, bonnet is the part in front of vehicles, thus will be the first part to reach the transmission range of overhead laser transmitters. And last, user seats are located under vehicles’ roofs, not under their bonnet, thus the safety of vehicle users under overhead laser-based OWPT is better when laser beams are pointed to the bonnet of ground EVs compared to that when laser beams are pointed to the roof of ground EVs.

Next, at the considering transmitting distance of less than 10 m and with clear atmospheric condition ( $\sigma = 0.1$  per km), the decrease of laser power expressed in the exponential term  $e^{-\sigma \ell}$  in (3) is ignorable, because  $e^{-\sigma \ell} \approx 1$ . As such, the accumulated wirelessly transmitted power is

$$P_c \approx 2P_\ell \eta_l \eta_e \int_0^{\varphi_m} \cos \varphi d\varphi = 2P_\ell \eta_l \eta_e \sin \varphi_m. \quad (11)$$

Accordingly, the amount of wirelessly transmitted energy to a ground EV is

$$E_c \approx nP_c \frac{2h \tan \varphi_m}{v_{wpt}} = 4nP_\ell \eta_l \eta_e \frac{h}{v_{wpt}} \tan \varphi_m \sin \varphi_m. \quad (12)$$

Thus, the wirelessly transmitted power and energy to a ground EV are monotonically increasing functions of the angle  $\varphi_m \in (0, \pi/2)$  and the distance  $h_i$ .

Finally, to fairly evaluate the proposed laser-based dynamic OWPT system, we attempt to compare it with the resonant IWPT technology for dynamic wireless charging of moving ground EVs on highways. Consider the same 400 kW rate power of the OWPT system as that for the lane using resonant IWPT [25], and assume that each laser transmitter has an output power of 2 kW, then there are 200 laser transmitters for the OWCL. Note that each laser transmitter can in fact be an array of smaller laser transmitters. Recent studies have tested kW-level laser beaming at the distances of tens of meters for OWPT, see e.g. [27]. The efficiency of optical lenses is assumed to be 95%. The height of a ground EV’s bonnet is assumed to be  $\approx 1.2$  m, and the angle  $\varphi_m$  is assumed to be  $\pi/4$ , hence  $h \approx 8.8$  m, and the total traveling distance of an EV while getting charged on the considering OWCL is  $200 \times 2h \tan \varphi_m = 3520$  m, i.e. 3.52 km. Additionally, it is assumed that the required speed on the wireless charging lane is  $v_{wpt} = 80$  km/h. The attenuation coefficient  $\sigma$  is typically 0.1 per km for clear air [23], as above. The conversion efficiency of solar cells on ground EVs is assumed to be 68.9%, similarly to that in Section III-D. Consequently, the total amount of energy a ground EV can get is as follows,

- From the proposed dynamic OWPT:  
 $3.52/80 \times 2 \times 400 \times 0.95 \times 0.689 \times \sin \frac{\pi}{4} = 16.2919$  kWh.

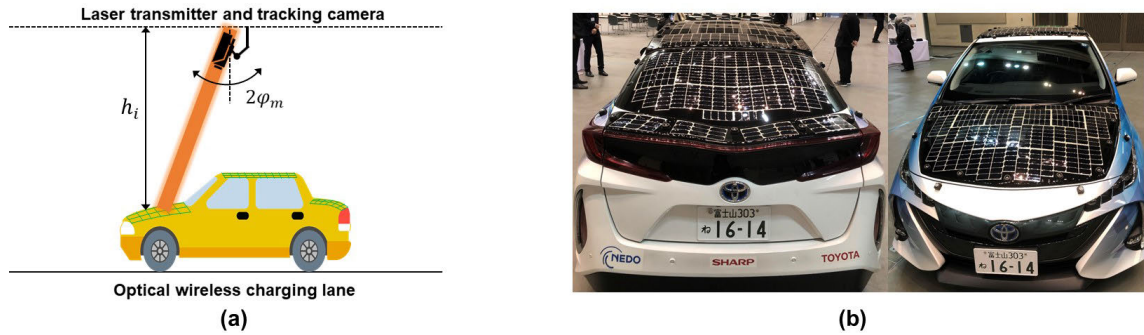


**FIGURE 5.** Illustration of the proposed laser-based dynamic OWPT for ground EVs via their bonnet-covered solar cells: (a) conceptual image; (b) a demo of hybrid EVs covered with solar cells developed in a NEDO-Toyota-Sharp project that could be fit for the concept.

- From the resonant IWPT, assumed its 90% efficiency and 95% efficiency of electronic circuits on EVs:  
 $3.52/80 \times 400 \times 0.95 \times 0.9 = 15.048 \text{ kWh}$ .

As seen, the amount of wireless charging energy received by the proposed laser-based dynamic OWPT is more than that by the resonant IWPT. Moreover, the proposed overhead laser-based dynamic OWPT can be employed for both moving ground and aerial EVs at much further transmitting distances than that in the range of tens of centimeters of the resonant IWPT technology. Therefore, if realized the proposed laser-based dynamic OWPT offers many advantages.

## V. CONCLUSION

A laser-based dynamic OWPT system is proposed in this paper for moving aerial and ground EVs. The proposed system consists of an overhead facility on which RESs such as solar panels or wind turbines are located to supply clean energy to laser transmitters. These overhead laser transmitters point downward and upward for wireless charging of ground and aerial EVs, respectively, while being able to rotate around the normal direction to charge EVs as they are moving. Consequently, mathematical formulas for characterizing the wirelessly transmitted power and energy are derived, based on which the maximum power and energy points are proved to uniquely exist in the determined intervals. Moreover, those extreme points are shown to be inversely linear functions of the environment attenuation coefficient. These results are then validated and illustrated by numerical simulations under different scenarios of weather conditions.

Next, the obtained theoretical results are utilized to provide hints for ground EVs design that are most suitable with the proposed dynamic OWPT system. More specifically, solar cells – the optical receivers should be attached to the bonnet of ground EVs in order to receive more energy from overhead laser transmitters. Additionally, the rotating angle of laser transmitters should be as big as possible for increasing the amounts of wirelessly transmitted power and energy.

The proposed system provides a novel approach of wireless charging multiple types of EVs (ground and aerial) while

they are moving, which is an advanced approach compared to traditional wired, static charging systems. As such, it is useful to push forward the decarbonization of the transportation sector. Simultaneously, it can also serve as an important infrastructure in smart grids and multi-energy systems, connecting EVs with power grids and other energy systems and providing ancillary services to the grids.

In the future works, experimental studies will be conducted to verify and confirm the proposed system and the derived theoretical results. Another line of research is to further develop the proposed system to enable OWPT-based bidirectional interconnection between EVs and the grid, since the current work allows only unidirectional power and energy flow from the grid to EVs.

## DECLARATIONS

The author declares no conflicts of interests on the work presented in this article.

## APPENDIX

We first prove the existence of a unique maximum power point. Let us denote

$$f(x) \triangleq x [\text{Ei}(-\alpha\sigma x) - \text{Ei}(-\sigma x)],$$

where  $\alpha > 1$  is a constant. Then  $P_{c,i} = 2P_{\ell}\eta_c \text{if}(h_i)$ , with the associated  $\alpha = 1/\cos \varphi_m$ .

Since  $\frac{\partial \text{Ei}(x)}{\partial x} = \frac{e^x}{x}$ , we have

$$\begin{aligned} \frac{\partial f(x)}{\partial x} &= \text{Ei}(-\alpha\sigma x) - \text{Ei}(-\sigma x) + x \left[ \frac{e^{-\alpha\sigma x}}{x} - \frac{e^{-\sigma x}}{x} \right] \\ &= \text{Ei}(-\alpha\sigma x) + e^{-\alpha\sigma x} - [\text{Ei}(-\sigma x) + e^{-\sigma x}]. \end{aligned} \quad (13)$$

Let  $g(x) \triangleq \text{Ei}(-x) + e^{-x}$ , then  $\frac{\partial f(x)}{\partial x} = g(\alpha\sigma x) - g(\sigma x)$ . Consequently, the derivative of  $g(x)$  can be computed to be

$$\frac{\partial g(x)}{\partial x} = \frac{e^{-x}}{x} - e^{-x} = \frac{(1-x)e^{-x}}{x}.$$

Hence,  $g(x)$  is a monotonically increasing function as  $x \in (0, 1]$ , whilst  $g(x)$  is a positive, monotonically decreasing function as  $x \in [1, +\infty)$ , and  $g(1) = \text{Ei}(-1) + e^{-1} \approx$

0.1485. As such, there exists a unique point  $x_0 \in (0, 1)$  such that  $g(x_0) = 0$ . Then we consider the following three cases.

- Case 1:  $0 < x \leq \frac{1}{\alpha\sigma} \Rightarrow \alpha\sigma x \leq 1, \sigma x < 1$ . We then obtain  $g(\alpha\sigma x) > g(\sigma x)$ , and hence,  $\frac{\partial f(x)}{\partial x} > 0$ . As a result,  $f(x)$  is a monotonically increasing function in this interval.

- Case 2:  $\frac{1}{\alpha\sigma} < x < \frac{1}{\sigma}$ . Taking the second partial derivative of  $f(x)$  with respect to  $x$  gives us,

$$\frac{\partial^2 f(x)}{\partial x^2} = \frac{e^{-\alpha\sigma x}}{x} \left[ 1 - \alpha\sigma x - (1 - \sigma x)e^{(\alpha-1)\sigma x} \right] < 0.$$

Hence,  $\frac{\partial f(x)}{\partial x}$  is a monotonically decreasing function in the interval  $(\frac{1}{\alpha\sigma}, \frac{1}{\sigma})$ . Furthermore,

$$\left. \frac{\partial f(x)}{\partial x} \right|_{x=\frac{1}{\alpha\sigma}} = g(1) - g(1/\alpha) > 0,$$

since  $g(x)$  is a monotonically increasing function as  $x \in (0, 1]$ , and

$$\left. \frac{\partial f(x)}{\partial x} \right|_{x=\frac{1}{\sigma}} = g(\alpha) - g(1) < 0,$$

because  $g(x)$  is a monotonically decreasing function as  $x \in [1, +\infty)$ . Thus, there must exist a unique point  $x^* \in (\frac{1}{\alpha\sigma}, \frac{1}{\sigma})$  such that  $\left. \frac{\partial f(x)}{\partial x} \right|_{x=x^*} = 0$ . In addition,  $\frac{\partial f(x)}{\partial x} > 0$  as  $x \in (\frac{1}{\alpha\sigma}, x^*)$ , and  $\frac{\partial f(x)}{\partial x} < 0$  as  $x \in (x^*, \frac{1}{\sigma})$ . As a result,  $f(x)$  is a monotonically increasing function in  $(\frac{1}{\alpha\sigma}, x^*)$ , while being a monotonically decreasing function in  $(x^*, \frac{1}{\sigma})$ .

- Case 3:  $x \geq \frac{1}{\sigma} \Rightarrow \alpha\sigma x > 1, \sigma x \geq 1$ . This leads to  $g(\alpha\sigma x) < g(\sigma x)$ , and hence,  $\frac{\partial f(x)}{\partial x} < 0$ . Thus,  $f(x)$  is a monotonically decreasing function.

Combining the results of all three cases above, we obtain that  $f(x)$  is a monotonically increasing and decreasing function in the interval  $(0, x^*)$  and  $(x^*, +\infty)$ , respectively. Obviously,  $x^*$  is the globally maximum point of  $f(x)$ . Finally, using this to  $P_{c,i}$  with  $\alpha = 1/\cos \varphi_m$  and let  $h^*$  be the point corresponding to  $x^*$  above, we obtain the maximum power point.

Next, we prove the existence of a unique maximum energy point. Denote

$$p(x) \triangleq x^2 [\text{Ei}(-\alpha\sigma x) - \text{Ei}(-\sigma x)],$$

where  $\alpha > 1$  is a constant. Then  $E_{c,i} = 4n_i P_\ell \eta_{c,i} \frac{\tan \varphi_m}{v_{wpt}} p(h_i)$ , with  $\alpha = 1/\cos \varphi_m$ .

We have

$$\begin{aligned} \frac{\partial p(x)}{\partial x} &= 2x [\text{Ei}(-\alpha\sigma x) - \text{Ei}(-\sigma x)] + x^2 \left[ \frac{e^{-\alpha\sigma x}}{x} - \frac{e^{-\sigma x}}{x} \right] \\ &= x [q(\alpha\sigma x) - q(\sigma x)], \end{aligned} \tag{14}$$

where  $q(x) \triangleq 2\text{Ei}(-x) + e^{-x}$ . The partial derivative of  $q(x)$  with respect to  $x$  is

$$\frac{\partial q(x)}{\partial x} = 2 \frac{e^{-x}}{x} - e^{-x} = \frac{(2-x)e^{-x}}{x}.$$

As such,  $q(x)$  is a monotonically increasing function as  $x \in (0, 2]$ , while being a positive, monotonically decreasing

function as  $x \in [2, +\infty)$ , and  $q(2) = 2\text{Ei}(-2) + e^{-2} \approx 0.0375$ . As such, there exists a unique point  $x_1 \in (0, 2)$  such that  $q(x_1) = 0$ .

- Case 1:  $0 < x \leq \frac{2}{\alpha\sigma} \Rightarrow \alpha\sigma x \leq 2, \sigma x < 2$ . This leads to  $q(\alpha\sigma x) > q(\sigma x)$ , and hence,  $\frac{\partial p(x)}{\partial x} > 0$ . Thus,  $p(x)$  is a monotonically increasing function in this interval.

- Case 2:  $\frac{2}{\alpha\sigma} < x < \frac{2}{\sigma}$ . Taking the partial derivative of  $q(\alpha\sigma x) - q(\sigma x)$  with respect to  $x$  yields,

$$\begin{aligned} &\frac{\partial (q(\alpha\sigma x) - q(\sigma x))}{\partial x} \\ &= \frac{e^{-\alpha\sigma x}}{x} \left[ 2 - \alpha\sigma x - (2 - \sigma x)e^{(\alpha-1)\sigma x} \right] < 0. \end{aligned}$$

Therefore,  $q(\alpha\sigma x) - q(\sigma x)$  is a monotonically decreasing function in the interval  $(\frac{2}{\alpha\sigma}, \frac{2}{\sigma})$ . Moreover,

$$(q(\alpha\sigma x) - q(\sigma x))|_{x=\frac{2}{\alpha\sigma}} = q(2) - q(2/\alpha) > 0,$$

since  $q(x)$  is a monotonically increasing function as  $x \in (0, 2]$ , and

$$(q(\alpha\sigma x) - q(\sigma x))|_{x=\frac{2}{\sigma}} = q(\alpha) - q(2) < 0,$$

because  $q(x)$  is a monotonically decreasing function as  $x \in [2, +\infty)$ . Hence, there must exist a unique point  $\tilde{x}^* \in (\frac{2}{\alpha\sigma}, \frac{2}{\sigma})$  such that  $(q(\alpha\sigma x) - q(\sigma x))|_{x=\tilde{x}^*} = 0$ . Additionally,  $q(\alpha\sigma x) - q(\sigma x) > 0$ , and hence,  $\frac{\partial p(x)}{\partial x} > 0$ , as  $x \in (\frac{2}{\alpha\sigma}, \tilde{x}^*)$ , whilst  $q(\alpha\sigma x) - q(\sigma x) < 0$ , and equivalently  $\frac{\partial p(x)}{\partial x} < 0$ , as  $x \in (\tilde{x}^*, \frac{2}{\sigma})$ . As such,  $p(x)$  is a monotonically increasing function in  $(\frac{2}{\alpha\sigma}, \tilde{x}^*)$ , while being a monotonically decreasing function in  $(\tilde{x}^*, \frac{2}{\sigma})$ .

- Case 3:  $x \geq \frac{2}{\sigma} \Rightarrow \alpha\sigma x > 2, \sigma x \geq 2$ . It can then be deduced that  $q(\alpha\sigma x) < q(\sigma x)$ , hence  $\frac{\partial p(x)}{\partial x} < 0$ , hence  $f(x)$  is a monotonically decreasing function.

Now, combining the results of all three cases above, we can deduce that  $p(x)$  is a monotonically increasing and decreasing function in the interval  $(0, \tilde{x}^*)$  and  $(\tilde{x}^*, +\infty)$ , respectively. It is also obvious that  $\tilde{x}^*$  is the globally maximum point of  $p(x)$ . Lastly, substituting this to  $E_{c,i}$  with  $\alpha = 1/\cos \varphi_m$  and let  $\tilde{h}^*$  be the point corresponding to  $\tilde{x}^*$ , we get maximum energy point.

Finally, we prove the inversely linear relation of the extreme points to  $\sigma$ , the attenuation coefficient of the transmitting environment. As shown earlier,  $h^*$  satisfies  $g(\alpha\sigma h^*) - g(\sigma h^*) = 0$ . Let  $y = \sigma h^*$ , we have

$$g(\alpha y) - g(y) = 0. \tag{15}$$

For a given angle  $\varphi_m$ ,  $\alpha$  is a known positive constant, hence (15) has a unique, constant solution  $y^*$ . As such,  $h^* = y^*/\sigma$ , and we obtain statement (i). Statement (ii) can be proved similarly.

## REFERENCES

[1] D. Patil, M. K. Mcdonough, J. M. Miller, B. Fahimi, and P. T. Balsara, "Wireless power transfer for vehicular applications: Overview and challenges," *IEEE Trans. Transport. Electrification*, vol. 4, no. 1, pp. 3–36, Mar. 2018.



- [2] A. Y. S. Lam, K.-C. Leung, and V. O. K. Li, "Vehicular energy network," *IEEE Trans. Transport. Electric.*, vol. 3, no. 2, pp. 392–404, Jun. 2017.
- [3] P. Machura and Q. Li, "A critical review on wireless charging for electric vehicles," *Renew. Sustain. Energy Rev.*, vol. 104, pp. 209–234, Apr. 2019.
- [4] D. H. Nguyen and A. Chapman, "The potential contributions of universal and ubiquitous wireless power transfer systems towards sustainability," *Int. J. Sustain. Eng.*, vol. 14, no. 6, pp. 1780–1790, Nov. 2021.
- [5] W. Han, K. T. Chau, C. Jiang, W. Liu, and W. H. Lam, "Design and analysis of quasi-omnidirectional dynamic wireless power transfer for fly-and-charge," *IEEE Trans. Magn.*, vol. 55, no. 7, pp. 1–9, Jul. 2019.
- [6] S. Li and C. C. Mi, "Wireless power transfer for electric vehicle applications," *IEEE J. Emerg. Sel. Topics Power Electron.*, vol. 3, no. 1, pp. 4–17, Mar. 2015.
- [7] A. A. S. Mohamed and O. Mohammed, "Bilayer predictive power flow controller for bidirectional operation of wirelessly connected electric vehicles," *IEEE Trans. Ind. Appl.*, vol. 55, no. 4, pp. 4258–4267, Jul. 2019.
- [8] T. M. Mostafa, A. Muharam, and R. Hattori, "Wireless battery charging system for drones via capacitive power transfer," in *Proc. IEEE PELS Workshop Emerg. Technologies: Wireless Power Transf. (WoW)*, May 2017.
- [9] D. H. Nguyen, G. Tumen-Ulzii, T. Matsushima, and C. Adachi, "Performance analysis of a perovskite-based thing-to-thing optical wireless power transfer system," *IEEE Photon. J.*, vol. 14, no. 1, pp. 1–8, Feb. 2022.
- [10] D. H. Nguyen, T. Matsushima, C. Qin, and C. Adachi, "Toward thing-to-thing optical wireless power transfer: Metal halide perovskite transceiver as an enabler," *Frontiers Energy Res.*, vol. 9, Jun. 2021, Art. no. 679125.
- [11] K. Jin and W. Zhou, "Wireless laser power transmission: A review of recent progress," *IEEE Trans. Power Electron.*, vol. 34, no. 4, pp. 3482–3499, Apr. 2019.
- [12] B. Clerckx, R. Zhang, R. Schober, D. W. K. Ng, D. I. Kim, and H. V. Poor, "Fundamentals of wireless information and power transfer: From RF energy harvester models to signal and system designs," *IEEE J. Sel. Areas Commun.*, vol. 37, no. 1, pp. 4–33, Jan. 2019.
- [13] J. L. Gomez-Tornero, M. Poveda-Garcia, R. Guzman-Quiros, and J. C. Sanchez-Arnause, "Design of Ku-band wireless power transfer system to empower light drones," in *Proc. IEEE Wireless Power Transf. Conf. (WPTC)*, May 2016, pp. 1–4.
- [14] Y. Huo, X. Dong, T. Lu, W. Xu, and M. Yuen, "Distributed and multilayer UAV networks for next-generation wireless communication and power transfer: A feasibility study," *IEEE Internet Things J.*, vol. 6, no. 4, pp. 7103–7115, Aug. 2019.
- [15] H. Helmers, E. Lopez, O. Höhn, D. Lackner, J. Schön, M. Schauerte, M. Schachtner, F. Dimroth, and A. W. Bett, "68.9% efficient GaAs-based photonic power conversion enabled by photon recycling and optical resonance," *Phys. Status Solidi, Rapid Res. Lett.*, vol. 15, no. 7, 2021, Art. no. 2100113.
- [16] R. Manson. (2011). *Feasibility of Laser Power Transmission to a High-Altitude Unmanned Aerial Vehicle*. [Online]. Available: [https://www.rand.org/pubs/technical\\_reports/TR898.html](https://www.rand.org/pubs/technical_reports/TR898.html)
- [17] Ericsson and PowerLight Technologies. (2021). *Ericsson and PowerLight Demonstrate World's First Wireless Powered 5G Base Station*. [Online]. Available: <https://www.ericsson.com/en/news/2021/10/ericsson-and-powerlight-achieve-base-station-wireless-charging-breakthrough>
- [18] U.S. Naval Research Laboratory. (2019). *Power Transmitted Over Laser (PTROL) Project*. [Online]. Available: <https://www.nrl.navy.mil/Media/News/Article/2504007/researchers-transmit-energy-with-laser-in-historic-power-beaming-demonstration>
- [19] Powerlight Technologies. *Video Archive*. Accessed: Nov. 27, 2022. [Online]. Available: <https://powerlighttech.com/our-videos/>
- [20] N. Javed, N.-L. Nguyen, S. F. A. Naqvi, and J. Ha, "Long-range wireless optical power transfer system using an EDFA," *Opt. Exp.*, vol. 30, no. 19, pp. 33767–33779, Sep. 2022.
- [21] A. Mohammadnia, B. M. Ziapour, H. Ghaebi, and M. H. Khooban, "Feasibility assessment of next-generation drones powering by laser-based wireless power transfer," *Opt. Laser Technol.*, vol. 143, Nov. 2021, Art. no. 107283.
- [22] Q. Zhang, W. Fang, Q. Liu, J. Wu, P. Xia, and L. Yang, "Distributed laser charging: A wireless power transfer approach," *IEEE Internet Things J.*, vol. 5, no. 5, pp. 3853–3864, Oct. 2018.
- [23] I. I. Kim, B. McArthur, and E. J. Korevaar, "Comparison of laser beam propagation at 785 nm and 1550 nm in fog and haze for optical wireless communications," *Proc. SPIE*, vol. 4214, pp. 26–37, Feb. 2001.
- [24] I. F. D. Oliveira and R. H. C. Takahashi, "An enhancement of the bisection method average performance preserving minmax optimality," *ACM Trans. Math. Softw.*, vol. 47, no. 1, pp. 1–24, Mar. 2021.
- [25] D. H. Nguyen, "Electric vehicle—Wireless charging-discharging lane decentralized peer-to-peer energy trading," *IEEE Access*, vol. 8, pp. 179616–179625, 2020.
- [26] D. H. Nguyen, "A cooperative learning approach for decentralized peer-to-peer energy trading markets and its structural robustness against cyberattacks," *IEEE Access*, vol. 9, pp. 148862–148872, 2021.
- [27] Y. Gou, H. Wang, J. Wang, R. Niu, X. Chen, B. Wang, Y. Xiao, Z. Zhang, W. Liu, H. Yang, and G. Deng, "High-performance laser power converts for direct-energy applications," *Opt. Exp.*, vol. 30, no. 17, pp. 31509–31517, Aug. 2022.



**DINH HOA NGUYEN** (Senior Member, IEEE) received the Ph.D. degree from The University of Tokyo, in 2014. He is currently an Associate Professor with Kyushu University, Fukuoka, Japan. His research interests include the modeling, optimization, and control toward low-carbon and autonomous energy, transportation, and other interconnected complex systems, renewables and distributed energy resources, smart grid, intelligent transportation, multi-agent systems, artificial intelligence, and decentralized optimization.

• • •